Thin–Walled Structures 146 (2020) 106446

Contents lists available at ScienceDirect

Thin-Walled Structures

journal homepage: http://www.elsevier.com/locate/tws

Full length article

Experimental and analytical study on structural performance of polyurethane foam-filled built-up galvanized iron members

R. Sagadevan, B.N. Rao *

Structural Engineering Laboratory, Department of Civil Engineering, Indian Institute of Technology Madras, Chennai, Tamil Nadu, 600036, India

ARTICLE INFO

Keywords:
Composite member
Sandwich panel
Polyurethane foam
Flexure
Shear
Compression
Light-weight sandwich beam
Light-weight sandwich column
Thin-walled structure

ABSTRACT

The sandwich members are widely adopted in building structures in particular pre-engineered building (PEB) as cladding and roof members due to its light-weight and thermal properties. PEB based Polyurethane foam (PUF) insulated structure is an alternative to the conventional PEB. The PUF filled sandwich structural members significantly reduces the structural steel weight and improves thermal performance. In this study, experiments were carried out to evaluate the flexural, shear and axial compression performance of PUF filled built-up sandwich beam/column, and purlin members which are fabricated with cold-formed sections made of thin galvanized iron (GI) sheets. In total 22 specimens were tested, in which ten beam/column specimens and twelve purlin specimens. The tests were conducted both in bare and PUF filled frames (specimens). The experimental results revealed that the PUF core material prevents premature failures which are common in cold-formed members and enhances the structural performance. As the observed failure mechanisms were not in line with the conventional cold-formed steel members. Hence, the capacity estimation based on the design guidelines given in Indian standard (IS) 801: 1975 (working stress method) and European standard (EN) 1993-1-3: 2006 (limit state method) may not be appropriate as these standards are based on the effective cross-section area. In this study, the applicability of existing design guidelines given in IS 800: 2007 for the hot-rolled section is verified through the estimation of flexural, shear and axial compression capacity. The estimated capacity was found to be in good agreement with the experimental results. Also, this method of estimation is found to be very simple in comparison with conventional cold-formed steel member design guidelines.

1. Introduction

The PEB structures are being adopted all over the world, and the construction of PEB is in increasing trend due to its suitability for multiple usages such as living habitat with integrated services, storage yards, industrial buildings and sheds, aircraft hangers, warehouse etc. However, the PEB structures made of conventional hot rolled steel members leads to an increase in self-weight, thus increase in cost. In addition, it is not suitable for high altitude locations due to difficulties in fabrication and erection. Additional thermal insulations are required to maintain the temperature inside PEB, particularly at cold storage yards, industrial office buildings and defence building at high altitude which needs to meet climatic conditions. PEB based Polyurethane foam (PUF) insulated structure is an alternative to the conventional PEB which satisfies the thermal and structural requirements, as the PUF has a low weight and high thermal insulation properties. The structural members are made of GI sections and infilled with PUF which are lightweight structural members. Generally, the GI sections/members are manufactured with thin cold-rolled and close annealed (CRCA) sheets. The structural members made of cold-formed thin sheets are susceptible to localised premature failures such as local and/or distortional buckling of section/member and shear buckling of web members. Initially, the research was carried out on sandwich panels as cladding for buildings due to its many advantages such as superior structural efficiency, ease of erection, mass-production capabilities and thermal-insulation qualities [1,2]. Local buckling phenomena is common in sandwich panels similar to that of thin-walled members. However, the buckling resistivity capacity of the core material increases the load-carrying capacity of sandwich panels [1]. Guidelines to design the sandwich panels with flat or thin-walled cold-formed steel facings and rigid foamed insulating core as cladding to building system are developed based on the various experimental (full-scale tests), numerical (finite-strip, finite-layer, finite-prism approaches), and analytical (boundary-value approach) results [2].

* Corresponding author.
E-mail addresses: sagadevan.ceg@gmail.com (R. Sagadevan), bnrao@iitm.ac.in (B.N. Rao).

https://doi.org/10.1016/j.tws.2019.106446
Received 18 July 2019; Received in revised form 2 September 2019; Accepted 2 October 2019
Available online 18 October 2019

The flexural behaviour of composite sandwich beams was studied experimentally and found that the compression side sheet exhibits a softening nonlinearity while the tension side sheet showed a stiffening non-linearity behaviour with full-composite action [3]. In the same study, the experimental results were found to be in good agreement with the predictions from simple models by neglecting the contribution from the core. The sandwich panels made of PUF core and glass fibre reinforced polymer (GFRP) skins with ribs of various configuration was investigated for its flexural performance [4]. The experimental results showed that the ultimate strength of panels was equivalent to the reinforced concrete (RC) panels of the same size with 0.6–2.0% reinforcement ratio and the weight of panels were 9–14 times lesser than that of RC panels. In addition, this study showed that the capacity and stiffness of sandwich panels are highly influenced by the density of PUF core and configuration of ribs. The flexural stiffness of multi-layered sandwich panels made of fibre reinforced polymer facing sheets with PUF core was investigated through experiments and found that the stiffness of sandwich panel is influenced by the thickness of facing sheet and core [5]. The aluminium foam-filled stainless steel sandwich beam was tested under three-point bending to investigate the flexural behaviour and found that the strength and stiffness were influenced by the form [6]. The flexural behaviour of GFRP sandwich panels with different density of PUF core and types of ribs was studied through three and four-point bending test and suggested economic configuration [7]. Mechanical properties of sandwich panels made of polystyrene/cement mixed cores and thin cement sheet facings were found by flexural test and found that the properties highly depend on the outer cement face sheets' properties [8]. The shear and flexural behaviour of the layered sandwich beam (LSB) consists of multiple sandwich panels made of GFRP skins and Phenolic core and found that LSB can overcome the premature failures such as wrinkling and buckling of the composite skins and indentation failure [9]. The experimental and numerical studies on the sandwich panels with external steel facings and core as PUF, mineral wood and combination of both was carried out and reported that the flexural capacity of the sandwich panel with PUF is twice that of the panel with mineral wood [10]. Structural performance of PUF filled the sandwich panel with various facing materials such as gypsum, engineered wood or some composite materials was reviewed [11]. In the same study, it was identified that many key parameters affecting the structural behaviour of sandwich panels and reported the importance of the research on the sandwich panels as building structural elements. The key parameters are bending and shear behaviour, energy absorption and dynamic behaviour, edgewise and flatwise compressive/tensile behaviour and delamination/deboning issues.

Previous researches were mainly focused on the sandwich panels made of thin face sheets as cladding and roof member to the building. Also, many of these researchers were studied the panels' flexural behaviour alone. In this study, experiments were carried out to investigate the flexural, shear and axial compression performance of PUF filled built-up GI sandwich structural members. This research is mainly focused on the load-carrying capacity of the sandwich structural members (beam/column and purlin). The guidelines for the design of cold-formed steel sections are given in IS 801: 1975 (working stress method) [12] and EN 1993-1-3: 2006 (limit state method) [13]. These design guidelines are based on the effective cross-section area which depends on the local and/or distortional buckling of section/member. However, the current experimental study revealed that the PUF core is overcoming the local premature failures. Hence, in this study the applicability of existing design guidelines given in IS 800: 2007 [14] for hot-rolled sections was investigated through estimating the flexural, shear and axial compression capacity of these members.

2. Experimental programme

Experiments were carried out to study the behaviour of structural beam/column (hereafter denoted as a beam) and purlin members made of GI with PUF as infill material. The unit weight of PUF was 40 kg/m^3. The structural performance of the members was studied under various loading conditions, such as flexure, shear, and compression. The behaviour of structural members is expressed in terms of load versus displacement plot, and the results are compared using load-carrying capacity corresponding to the observed failure load.

2.1. Details of test specimens

The GI members (main profile and cross angle) were CRCA sheet of 1.2 mm thickness with design strength of 250 N/mm^2. The members were laminated with 0.45 mm thickness pre-coated galvanized iron (PCGI) sheet to facilitate the filling of PUF. The PUF material is flammable and may produces toxic gases with fire [15,16]. Although PUF is susceptible to produce toxic gases with fire, standard building codes recommend a minimum of 0.4 mm thickness of steel sheets as metal facing to the PUF core to increase the fire-resisting capacity, and to reduce the production and leaking of toxic gases during an unfavourable event of fire [17]. Accordingly, in this study, PCGI sheet of 0.45 mm thickness was adopted as metal facing to the PUF core. The PCGI sheets had micro serration to increase the bond with PUF. The beam members have a main profile at top and bottom which were connected by cross angle members forming truss type structure. A portion of a bare beam member is shown in Fig. 1.

Full scale specimens were tested, which are representing various structural members (column, beam, and purlin) of a PEB as shown in Fig. 2(a). In total 22 specimens were tested. The members' section details such as dimensions, the arrangement of main profile and cross angle, PUF details, etc., are shown in Fig. 2(b) and (c) and The details of test specimens are summarised in Table 1. Flexural tests on beam members were carried out in both minor and major axis to understand its complete behaviour.

2.2. Experimental test setup and instrumentation

2.2.1. Test setup

2.2.1.1. Flexure. Four-point bending test was conducted to study the flexural behaviour of structural members made of GI with PUF as infill material. Fig. 3(a) shows the schematic test set-up. Fig. 3(b) and (c) show the photographs of the test set-up with specimens F–B1–BF-XX and F–B2–F/PUF-XX, respectively. Steel plate of size 300 mm × 300 mm × 16 mm was used for load transfer (except for specimen F–P2–F/PUF-YY) as patch load to avoid localised pre-mature failure. The adopted steel plate size for the specimen F–P2–F/PUF-YY was 300 mm × 600 mm × 23 mm, as it was tested for minor axis bending and the width of the specimen was 450 mm. Hydraulic machine of 400 kN capacity was used to apply the load. The specimens were supported by a hinge at one end and roller at the other end at their edges, which is located 150 mm from specimen edges.

2.2.1.2. Shear. The three-point test was conducted to study the shear behaviour of structural members made of GI with PUF as infill material.

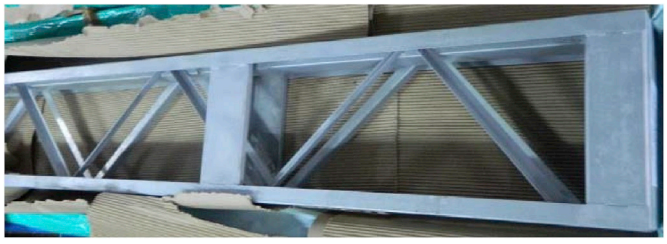

Fig. 1. A portion of bare beam member.

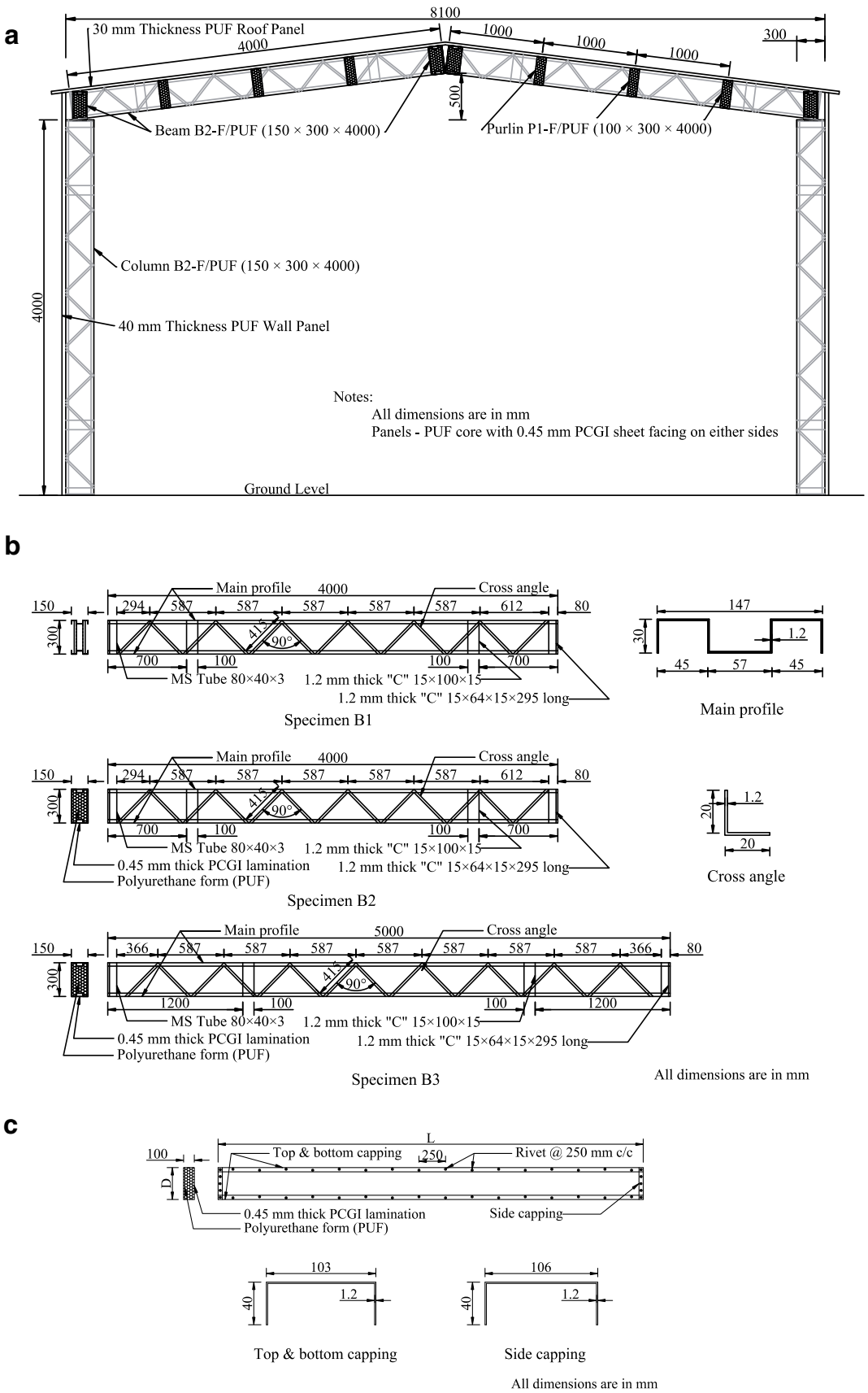

Fig. 2. a)Typical frame details of a PEB, b)Details of beam specimens (B1, B2, and B3), c)Details of purlin specimens (P1, P2, P3, and P4).

Table 1
Details of test specimens.

Sl. No.	Specimen ID	Dimension, mm (B × D × L)	Self-weight, kN	Test
1	F–B1–BF-XX	150 × 300 × 4000	0.33	Flexure – major axis
2	F-B1-BF-YY	150 × 300 × 4000	0.33	Flexure – minor axis
3	F–B2–F/PUF-XX	150 × 300 × 4000	0.53	Flexure – major axis
4	F–B2–F/PUF-YY	150 × 300 × 4000	0.53	Flexure – minor axis
5	S–B1–BF	150 × 300 × 4000	0.33	Shear
6	S–B2–F/PUF-1	150 × 300 × 4000	0.53	Shear
7	S–B2–F/PUF-2	150 × 300 × 4000	0.53	Shear
8	C–B1–BF	150 × 300 × 4000	0.33	Axial compression
9	C–B2–F/PUF	150 × 300 × 4000	0.53	Axial compression
10	C–B3–F/PUF	150 × 300 × 5000	0.66	Axial compression
11	F–P1–F/PUF-XX	100 × 300 × 4000	0.29	Flexure – major axis
12	F–P1–F/PUF-YY	100 × 300 × 4000	0.29	Flexure – minor axis
13	F–P2–F/PUF-XX	100 × 450 × 4000	0.43	Flexure – major axis
14	F–P2–F/PUF-YY	100 × 450 × 4000	0.43	Flexure – minor axis
15	S–P1–F/PUF-1	100 × 300 × 4000	0.29	Shear
16	S–P1–F/PUF-2	100 × 300 × 4000	0.29	Shear
17	S–P2–F/PUF-1	100 × 450 × 4000	0.43	Shear
18	S–P2–F/PUF-2	100 × 450 × 4000	0.43	Shear
19	C–P1–F/PUF	100 × 300 × 4000	0.29	Axial compression
20	C–P2–F/PUF	100 × 450 × 4000	0.43	Axial compression
21	C–P3–F/PUF	100 × 300 × 5000	0.36	Axial compression
22	C–P4–F/PUF	100 × 450 × 5000	0.54	Axial compression

Note: F – flexure, S – shear, C – axial compression, B1, B2, and B3 – beam specimens 1, 2 and 3 (based on dimension and presence of infill), P1, P2, P3, and P4 – purlin specimens 1, 2, 3, and 4 (based on dimension), BF – bare frame, F/PUF – frame in-filled with Polyurethane foam, XX – flexural test about major axis, and YY – flexural test about minor axis.

Fig. 4(a) and (b) shows the schematic and actual test set-up, respectively. The load was applied through steel plate of size 200 mm × 410 mm × 16 mm as patch load to avoid localised pre-mature failure. Hydraulic machine of 400 kN capacity was used to apply the load. The specimens were supported by a hinge at one side and roller at the other side which were located at a distance equal to the depth of specimen from point of application of load.

2.2.1.3. Axial compression. The axial load test was conducted to study the compression behaviour of structural members made of GI with PUF as infill material. Fig. 5(a) and (b) shows the schematic and actual test set-up, respectively. Hydraulic machine of 6000 kN capacity was used to apply the load. The ends of the member were not allowed to translate as well as rotate.

2.2.2. Instrumentation

Inbuilt load gauge of the hydraulic machine was utilised for the load measurement for flexure and shear tests. For axial compression test, the applied load was measured using 1000 kN capacity load cell, as the expected specimen capacity was much lesser than hydraulic machine capacity. For the flexural test, three linear variable differential transformers (LVDTs) with a measurement range of ±100 mm were used to measure the displacements at mid-span and under the point of application of loads (except for specimen F–B2–F/PUF-YY). For the specimen F–B2–F/PUF-YY, the displacements were measured at mid-span and at a distance of 670 mm on either side from the centre of the span. For axial compression test, three LVDTs with a measurement range of ±100 mm were used to measure the lateral displacements at a distance of 1000 mm, 2000 mm, and 3000 mm from the base of the column specimen. Fig. 3(a) and Fig. 5(a) shows the schematic arrangement of LVDTs. A data acquisition system was used to obtain real-time experimental data which has the facility to record the load and displacement simultaneously. Load controlled monotonic test was performed. The test was terminated immediately after observing a major drop in applied load; it ensures the safety of measuring and loading devices.

3. Experimental results and discussions

3.1. Load displacement behaviour

3.1.1. Flexure

All specimens tested under four-point load showed typical flexural failure. Observed load versus mid-span displacement behaviour of bare frame specimen (F–B1–BF) and specimen in-filled with PUF (F–B2–F/PUF) shows that the load-carrying capacity and flexural stiffness are higher for in-filled with PUF specimen (Fig. 6). It needs to be noted that the bare frame specimen (F–B1–BF) was failed prematurely by buckling of cross angle (diagonal member) and it was avoided in the specimen F–B2–F/PUF which is attributed to the presence of PUF. Similarly, the increase in load-carrying capacity and stiffness of purlin, P2 in comparison with purlin, P1 was observed, which is attributed to the increase in overall depth (Fig. 7). As expected, the flexural capacity and stiffness of beam and purlin members about the minor axis are lower than that of major axis bending. The observed load versus displacement for each tested specimens is shown in Fig. 8.

3.1.2. Axial compression

All specimens tested under axial compression showed either global buckling or localised failure, such as buckling of the main profile, crippling/crushing at ends. The observed load versus lateral displacement for each tested specimens is shown in Fig. 9. In Fig. 9, few lateral displacement (LVDT) data are not reported as those LVDT were malfunctioned during the test. By comparing the load-carrying capacity of bare frame specimen (C–B1–BF) and specimen in-filled with PUF (C–B2–F/PUF), it is observed that the load-carrying capacity is 65% higher for specimen in-filled with PUF. The bare frame specimen (*C*–B1–BF) was failed prematurely by local buckling of the main profile and it was avoided in the specimen C–B2–F/PUF which is attributed to the presence of PUF. In the purlin members, the crushing of loading end was observed to predominant failure than buckling.

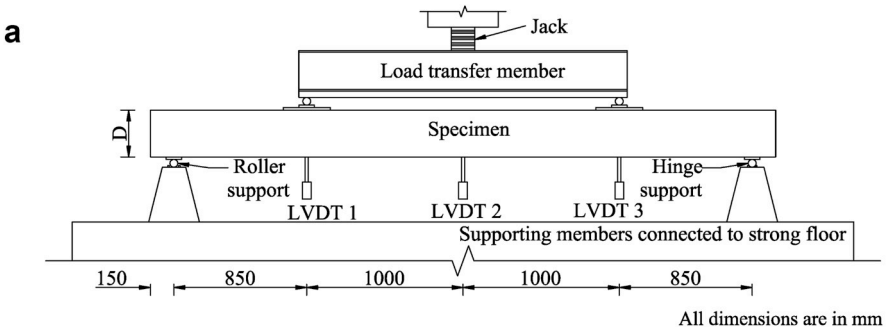

Fig. 3. a)Schematic experimental test set-up: flexure, b)Photograph of experimental test set-up: flexure (specimen: F–B1–BF-XX), c)Photograph of experimental test set-up: flexure (specimen: F–B2–F/PUF-XX).

a

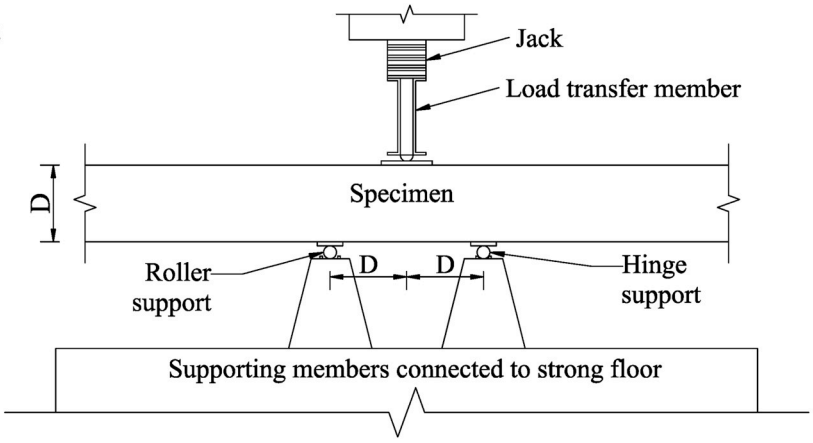

b

Fig. 4. a)Schematic experimental test set-up: shear, b)Photograph of experimental test set-up: shear.

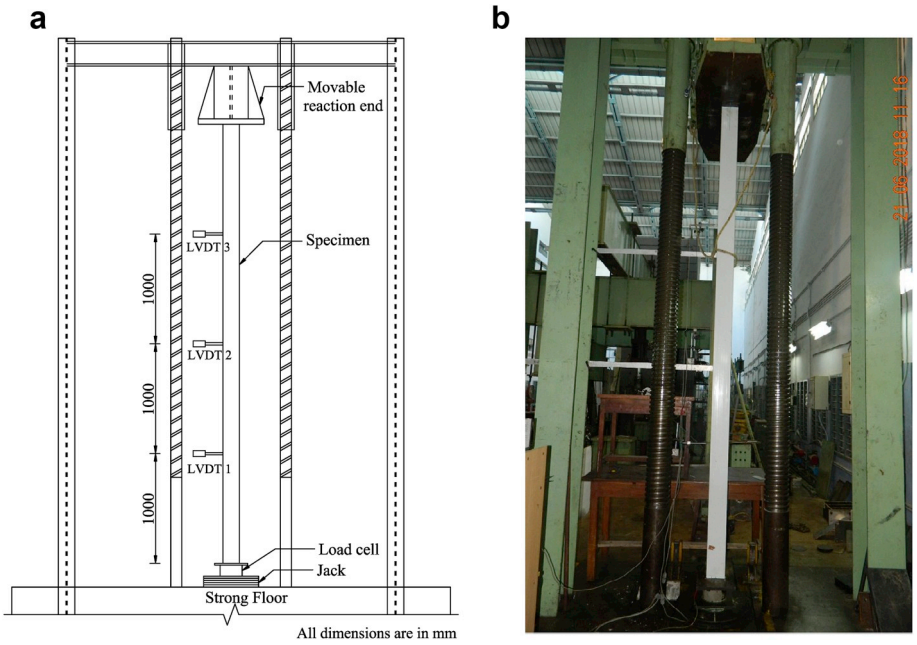

Fig. 5. a)Schematic experimental test set-up: axial compression, b)Photograph of experimental test set-up: axial compression.

3.2. Load carrying capacity

3.2.1. Flexure

The failure load and corresponding mid-span displacement are summarised for all tested specimens in Table 2. From the test results of beam specimens B1 and B2, it is observed that the load-carrying capacity of specimen B2 (filled with PUF) is more than twice that of specimen B1 (bare frame) in both axes of bending. The increase in load-carrying capacity is attributed to the PUF infill which helps to avoid premature localised failure. The ratio between load-carrying capacity and self-weight is in the range of 30–98.5 and 33–129 for beams and purlins, respectively, which is highly appreciable. Typical specimen failure is shown in Fig. 10 for specimens F–B1–BF-XX and F–B2–F/PUF-XX.

3.2.2. Shear

Table 3 comprises the failure load for all tested specimens. From the test results of beam specimens B1 and B2, it is observed that the shear load carrying capacity of specimen B2 (filled with PUF) is almost thrice that of specimen B1 (bare frame). The increase in load-carrying capacity is attributed to the PUF infill, which helps to avoid premature localised failure. Typical specimen failure is depicted in Fig. 11 for specimens S–B1–BF and S–B2–F/PUF-1.

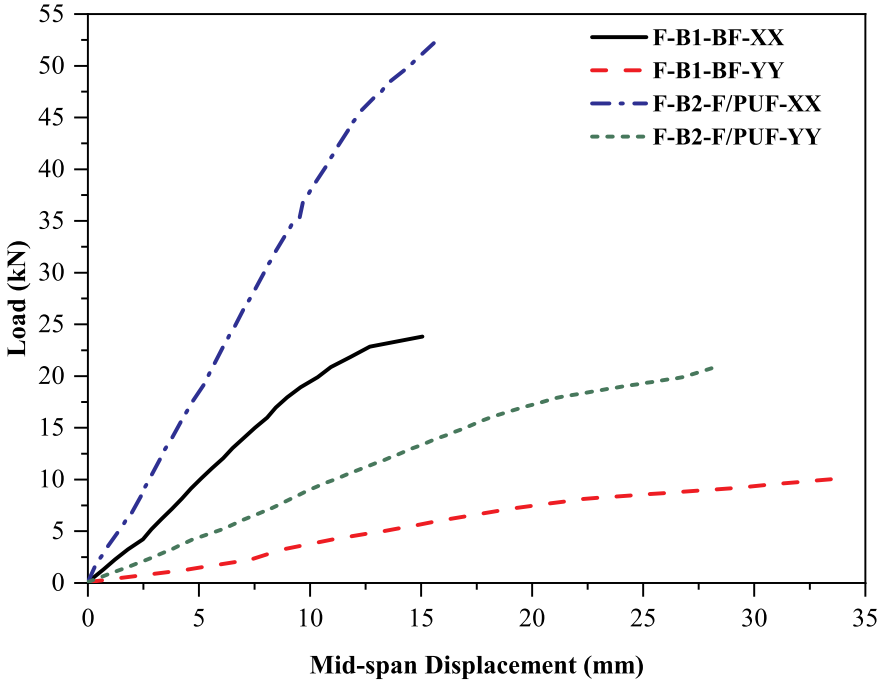

Fig. 6. Load versus mid-span displacement of beam specimens.

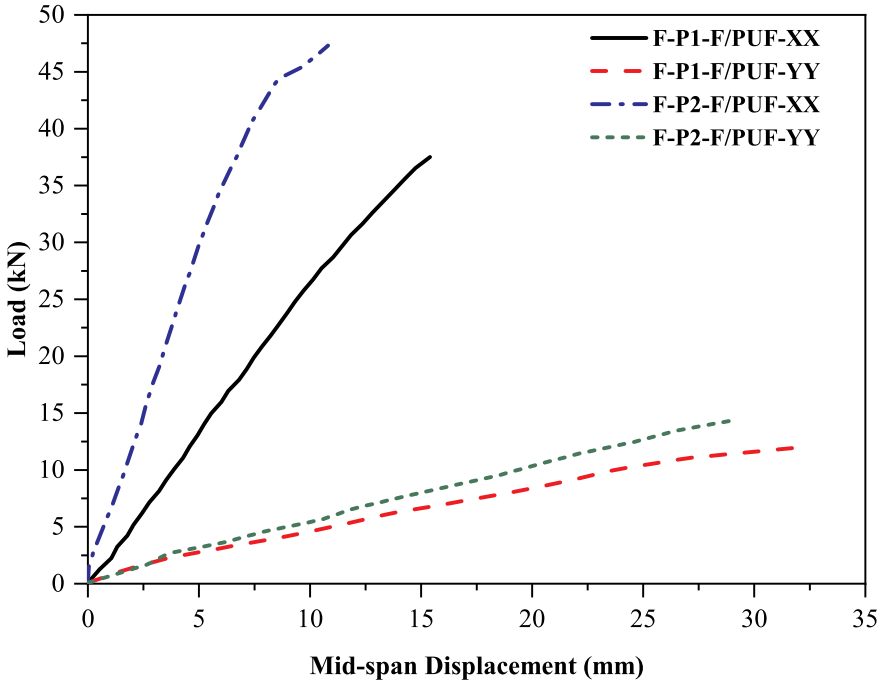

Fig. 7. Load versus mid-span displacement of purlin specimens.

3.2.3. Axial compression

Observed failure load is summarised for all tested specimens in Table 4. From the test results of beam specimens B1 and B2, it is observed that the axial load carrying capacity of specimen B2 (filled with PUF) is almost twice that of specimen B1 (bare frame). The increase in load-carrying capacity is attributed to the PUF infill which helps to avoid premature localised failure. As expected, the increase in height reduces the axial load carrying capacity of the beam member. However, it is not observed in purlin members, which is attributed to the localised crushing of member at loading end prior to buckling mode of failure. Typical specimen failure is shown in Fig. 12 for specimens C–B1–BF and C–B2–F/PUF.

4. Prediction of capacity

The beam and purlin members which are considered in this study were made of thin sections. The beam member section has thin angle section as web and the webs susceptible to shear buckling before yielding. This phenomenon was observed in experiments as well. Hence, the following assumption is made in accordance with IS 800: 2007. The bending (flexure) moment and axial force acting on the section is assumed to be resisted by flanges only and the shear force resisted by web members alone. However, for the purlin members, the shear capacity is estimated based on the channel lips only as it does not have a web. The presence of PUF material is ignored conservatively for capacity estimation. The guidelines for the design of cold-formed steel sections are given in IS 801: 1975 [12] and EN 1993-1-3: 2006 [13]. These design guidelines are based on the effective cross-section area which depends on the local and/or distortional buckling of section/member. However, in this study, the structural beam and purlin members are filled with PUF. The PUF infill helps to avoid premature localised failure, such as local and/or distortional buckling of section/member and ensures global member failure mainly by the bonding of PUF with GI member and PCGI facing sheet. Hence the conventional design guidelines are given in IS 800: 2007 [14] for hot-rolled sections are adopted in this study. The details of the design guidelines are summarised below for all three behaviours such as flexure, shear, and axial compression. The estimated capacity of various sections is compared with experimental observations to verify the applicability of the adopted guidelines to design the members with PUF infill.

4.1. Flexure

The bending strength (M_n) of a section can be estimated by Eq. (1a). The estimated capacity is summarised in Table 5.

$$M_n = \beta_b Z_p f_y \leq 1.2 Z_e f_y \tag{1a}$$

where, Z_p and Z_e are plastic and elastic section modulus of the cross-section, respectively, f_y is yield stress of the material, and β_b is constant depends on the class of section, given by Eq. (1b).

$$\beta_b = \begin{cases} 1.0 & \text{for plastic and compact sections} \\ Z_e/Z_p & \text{for semi} - \text{compact sections} \end{cases} \tag{1b}$$

The design bending strength (M_d) of a section can be estimated by Eq. (1c).

$$M_d = M_n/\gamma_{m0} \tag{1c}$$

where, γ_{m0} is partial safety factor (= 1.1). For the purpose of comparison of estimated capacity with experimental results, the partial safety factor for the material is taken as one.

From Table 5, it can be seen that the prediction matches with the experimental observations closely except for member without PUF infill (B1). The difference in capacity attributed to the unintended premature failure of bare frame (B1).

4.2. Shear

The shear capacity (V_n) of a section can be estimated by Eq. (2a). The estimated shear capacity is summarised in Table 6.

$$V_n = A_v f_{yw} \Big/ \sqrt{3} \tag{2a}$$

where, A_v is shear area, and f_{yw} is yield strength of the web. The design

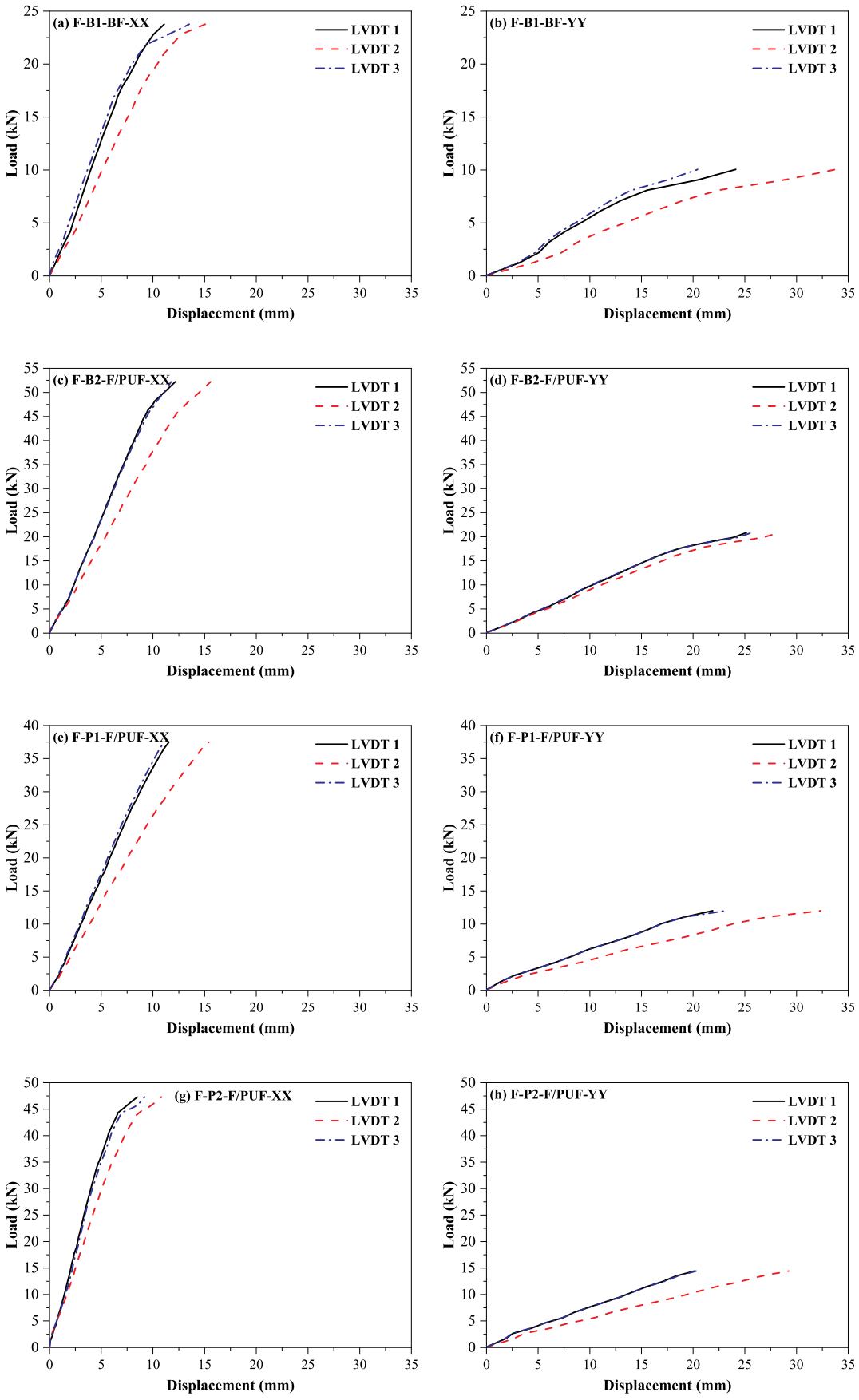

Fig. 8. Load versus displacement of tested specimens (flexure).

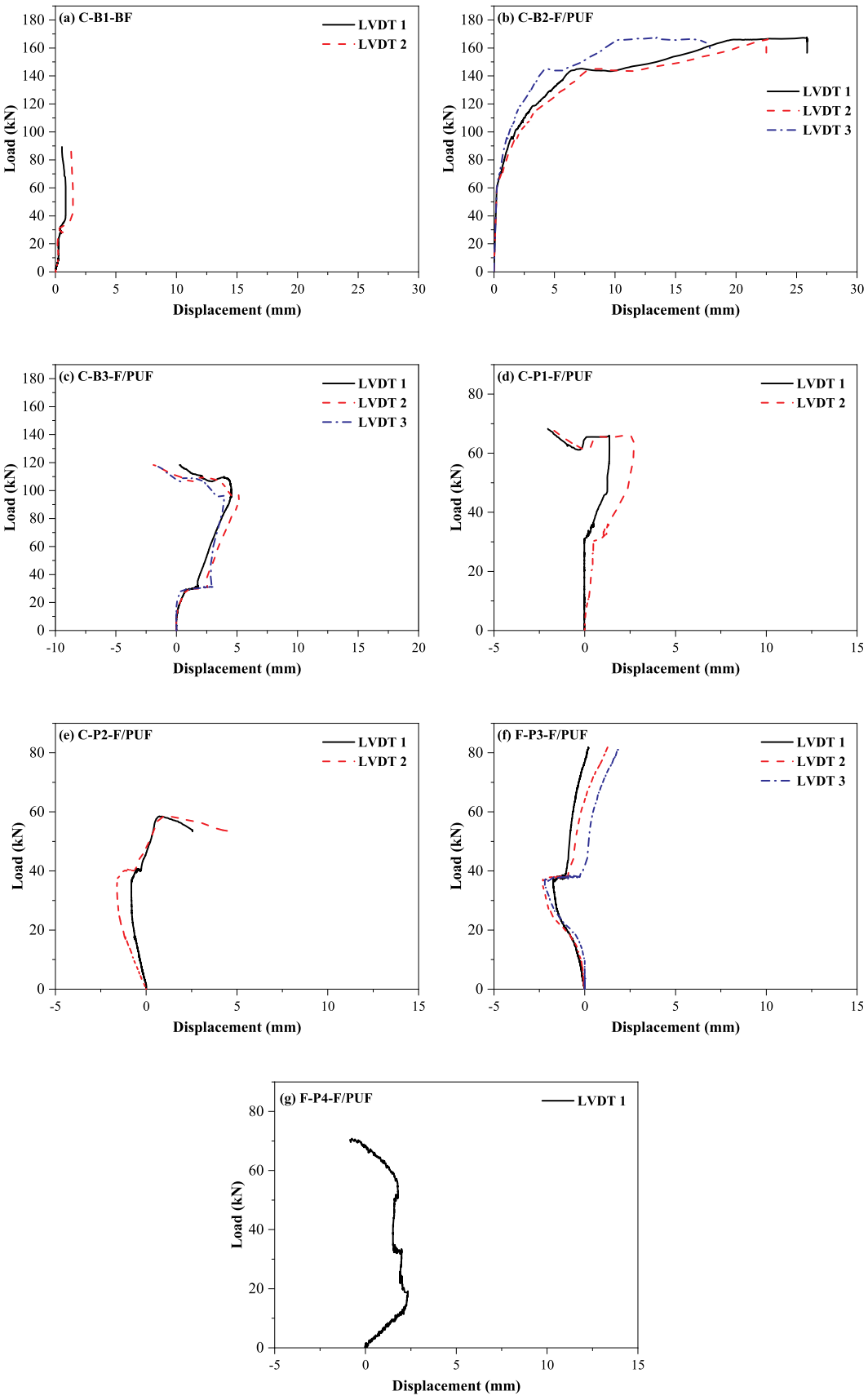

Fig. 9. Load versus displacement of tested specimens (axial compression).

Table 2
Experimental results: flexure.

Sl. No.	Specimen ID	Self-weight (W_{DL}), kN	Failure load (P_{uf}), kN	At mid-span		Ratio, P_{uf}/W_{DL}
				Displacement (δ_u), mm	Moment (M_u), kN-m	
1	F–B1–BF-XX	0.33	23.77	15.08	10.25	72.03
2	F-B1-BF-YY	0.33	10.03	33.84	4.42	30.39
3	F–B2–F/PUF-XX	0.53	52.22	15.60	22.44	98.53
4	F–B2–F/PUF-YY	0.53	20.82	28.29	9.09	39.28
5	F–P1–F/PUF-XX	0.29	37.50	15.42	16.07	129.31
6	F–P1–F/PUF-YY	0.29	11.99	32.39	5.23	41.34
7	F–P2–F/PUF-XX	0.43	47.31	10.83	20.31	110.02
8	F–P2–F/PUF-YY	0.43	14.37	29.27	6.31	33.42

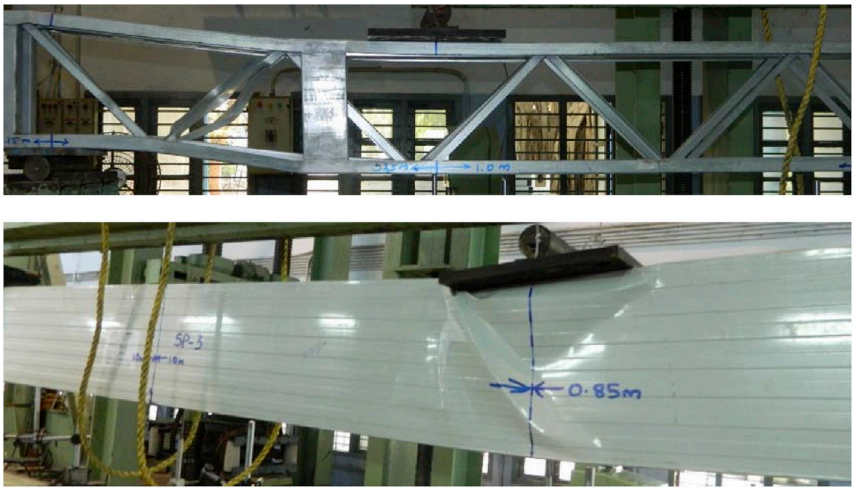

Fig. 10. Observed failure of specimens F–B1–BF-XX and F–B2–F/PUF-XX (flexure).

shear capacity (V_d) of a section can be estimated by Eq. (2b).

$$V_d = V_n/\gamma_{m0} \tag{2b}$$

where, γ_{m0} is partial safety factor (= 1.1). For the purpose of comparison of estimated capacity with experimental results, the partial safety factor for the material is taken as one.

4.3. Axial compression

The axial compression capacity (P_n) of member can be estimated by Eq. (3a). The estimated axial load capacity is summarised in Table 7.

$$P_n = \frac{A_e f_y}{\phi + \sqrt{\phi^2 - \lambda^2}} \le A_e f_y \qquad \text{Eq. (3a)}$$

where, A_e is effective sectional area, f_y is yield stress of the material, φ is constant given by Eq. (3b), and λ is non-dimensional effective slenderness ratio, given by Eq. (3c).

$$\phi = 0.5\left[1 + \alpha(\lambda - 0.2) + \lambda^2\right] \tag{3b}$$

$$\lambda = \sqrt{f_y \left(KL/r\right)^2 \Big/ \pi^2 E} \tag{3c}$$

where, α is imperfection factor (= 0.49 for built-up member), KL is effective length of column ($K = 0.65$ for column with translation and rotation restrained ends), r is radius of gyration of section, and E is the modulus of elasticity (= 2×10^5 N/mm^2). The design axial compression capacity (P_d) of column member can be estimated by Eq. (3d).

$$P_d = P_n/\gamma_{m0} \tag{3d}$$

where, γ_{m0} is partial safety factor (= 1.1). For the purpose of comparison of estimated capacity with experimental results, the partial safety factor for the material is taken as one.

Table 3
Experimental results: shear.

Sl. No.	Specimen ID	Failure load, kN	Mean failure load, kN	Shear capacity (V_u), kN
1	S–B1–BF	24.52	24.52	12.26
2	S–B2–F/PUF-1	76.02	72.34	36.17
3	S–B2–F/PUF-2	68.67		
4	S–P1–F/PUF-1	40.22	40.71	20.35
5	S–P1–F/PUF-2	41.20		
6	S–P2–F/PUF-1	43.16	46.10	23.05
7	S–P2–F/PUF-2	49.05		

Fig. 11. Observed failure of specimens S–B1–BF and S–B2–F/PUF (shear).

Table 4
Experimental results: axial compression.

Sl. No.	Specimen ID	Self-weight (W_{DL}), kN	Failure load (P_u), kN	Ratio, P_u/W_{DL}
1	C–B1–BF	0.33	89.55	271.36
2	C–B2–F/PUF	0.53	168.35	317.64
3	C–B3–F/PUF	0.66	118.87	180.11
4	C–P1–F/PUF	0.29	71.16	245.38
5	C–P2–F/PUF	0.43	82.60	192.09
6	C–P3–F/PUF	0.36	88.65	246.25
7	C–P4–F/PUF	0.54	80.98	149.96

Fig. 12. Observed failure of specimens C–B1–BF and C–B2–F/PUF (axial compression).

Table 5
Comparison of experimental and theoretical moment capacity.

Sl. No.	Specimen ID	Experimental moment (M_u), kN-m	Section modulus, mm^3		Estimated moment (M_n), kN-m	Ratio, M_u/M_n
			Elastic, Z_e	Plastic, Z_p		
1	F–B1–BF-XX	10.25	79126	86093	19.78	0.52
2	F-B1-BF-YY	4.42	20103	26900	5.02	0.88
3	F–B2–F/PUF-XX	22.44	79126	86093	19.78	1.13
4	F–B2–F/PUF-YY	9.09	20104	26900	5.02	1.81
5	F–P1–F/PUF-XX	16.07	57730	61031	14.43	1.11
6	F–P1–F/PUF-YY	5.23	13613	15845	3.40	1.54
7	F–P2–F/PUF-XX	20.31	90010	93539	22.50	0.90
8	F–P2–F/PUF-YY	6.31	13613	15845	3.40	1.86
Based on the specimens tested with PUF infill				Mean		1.39
				Standard deviation		0.37

Table 6
Comparison of experimental and theoretical shear capacity.

Sl. No.	Specimen ID	Experimental shear capacity (V_u), kN	Web area (A_v), mm^2	Estimated shear capacity (V_n), kN	Ratio, V_u/V_n
1	S–B1–BF	12.26	93.12	13.44	0.91
2	S–B2–F/PUF	36.17	93.12	13.44	2.69
3	S–P1–F/PUF	20.35	155.2	22.40	0.91
4	S–P2–F/PUF	23.05	155.2	22.40	1.03

Table 7
Comparison of experimental and theoretical axial compression capacity.

Sl. No.	Specimen ID	Experimental capacity (P_u), kN	Sectional area (A_e), mm^2	Effective slenderness ratio (KL/r)	Estimated capacity (P_n), kN	Ratio, P_u/P_n
1	C–B1–BF	89.55	629.28	53.66	123.20	0.73
2	C–B2–F/PUF	168.35	629.28	53.66	123.20	1.37
3	C–B3–F/PUF	118.87	629.28	67.07	108.63	1.09
4	C–P1–F/PUF	71.16	433.44	64.65	76.67	0.93
5	C–P2–F/PUF	82.60	433.44	80.81	64.37	1.28
6	C–P3–F/PUF	88.65	433.44	64.65	76.67	1.16
7	C–P4–F/PUF	80.98	433.44	80.81	64.37	1.26
Based on the specimens tested with PUF infill				Mean		1.18
				Standard deviation		0.14

From Table 7, it can be seen that the predicted axial compression capacity is closely matched with the experimental observations. For specimens with PUF infill, the under-estimation of capacity (flexure, shear and axial compression) is attributed to strain hardening in the galvanized iron. Since the guidelines of the building standards are based on the yield strength and do not account for effect of strain hardening in galvanized iron, the predictions based on the recommendations of the codes usually turn out to be conservative, which is observed in this study as well.

5. Summary and conclusions

The structural performance of built-up beam/column and purlin members made of galvanized iron (GI) with Polyurethane foam (PUF) as infill material is investigated in this study through flexural, shear and axial compression tests. In total 22 specimens were tested. The applicability of existing design guidelines given in IS 800: 2007 is verified. Following conclusions are arrived based on the experimental and theoretical study on the structural performance of built-up members.

1. The flexural capacity of specimen filled with PUF (B2) is more than twice that of bare frame specimen (B1) in both axes of bending.
2. Shear capacity of specimen filled with PUF (B2) is almost thrice that of bare frame specimen (B1).
3. Axial compression capacity of specimen filled with PUF (B2) is almost twice that of bare frame specimen (B1).
4. The increase in load-carrying capacity is attributed to the PUF infill which helps to avoid premature localised failure, such as local and/or distortional buckling of section/member.
5. The capacity (flexure, shear and axial compression) prediction by the guidelines given in IS 800: 2007 for the hot-rolled section is closely matched with experimental observations. It evidences that the capacity of built-up structural members made of galvanized iron (GI) with Polyurethane foam (PUF) as infill material can be estimated by the provisions of IS 800: 2007.

Acknowledgement

This work was supported by M/s Rinac India Limited, Bangalore, India. The authors wish to acknowledge the assistance and facilities offered by Technical Staff, Structural Engineering Laboratory, IIT Madras.

Appendix A. Supplementary data

Supplementary data to this article can be found online at https://doi.org/10.1016/j.tws.2019.106446.

References

[1] J.M. Davies, Sandwich Panels, Thin-Walled Structures, vol. 16, 1993, pp. 179–198, https://doi.org/10.1016/0263-8231(93)90044-B.
[2] K.P. Chong, J.A. Hartsock, Structural analysis and design of sandwich panels with cold-formed steel facings, Thin-Walled Struct. 16 (1993) 199–218, https://doi.org/10.1016/0263-8231(93)90045-C.
[3] I.M. Daniel, J.L. Abot, Fabrication, testing and analysis of composite sandwich beams, Compos. Sci. Technol. 60 (2000) 2455–2463, https://doi.org/10.1016/S0266-3538(00)00039-7.

[4] A. Fam, T. Sharaf, Flexural performance of sandwich panels comprising Polyurethane core and GFRP skins and ribs of various configurations, Compos. Struct. 92 (2010) 2927–2935, https://doi.org/10.1016/j.compstruct.2010.05.004.
[5] M. Vijay Kumar, B. Soragaon, Fabrication and evaluation of multilayered Polyurethane foam core sandwich panels for static flexural stiffness, Procedia Eng. 97 (2014) 1227–1236, https://doi.org/10.1016/j.proeng.2014.12.401.
[6] L.L. Yan, B. Han, B. Yu, C.Q. Chen, Q.C. Zhang, T.J. Lu, Three-point bending of sandwich beams with aluminum foam-filled corrugated cores, Mater. Des. 60 (2014) 510–519, https://doi.org/10.1016/j.matdes.2014.04.014.
[7] H. Tuwair, M. Hopkins, J. Volz, M.A. ElGawady, M. Mohamed, K. Chandrashekhara, V. Birman, Evaluation of sandwich panels with various Polyurethane foam-cores and ribs, Compos. B Eng. 79 (2015) 262–276, https://doi.org/10.1016/j.compositesb.2015.04.023.
[8] H.R. Tabatabaiefar, B. Mansoury, M.J.K. Zand, D. Potter, Mechanical properties of sandwich panels constructed from polystyrene-cement mixed cores and thin cement sheet facings, J. Sandw. Struct. Mater. 19 (2017) 456–481, https://doi.org/10.1177/1099636215621871.
[9] W. Ferdous, A. Manalo, T. Aravinthan, A. Fam, Flexural and shear behaviour of layered sandwich beams, Constr. Build. Mater. 173 (2018) 429–442, https://doi.org/10.1016/j.conbuildmat.2018.04.068.
[10] R. Studziński, Z. Pozorski, Experimental and numerical analysis of sandwich panels with hybrid core, J. Sandw. Struct. Mater. 20 (2018) 271–286, https://doi.org/10.1177/1099636216646789.
[11] B. Samali, S. Nemati, P. Sharafi, F. Tahmoorian, F. Sanati, Structural performance of Polyurethane foam-filled building composite panels: a state-of-the-art, J. Compos. Sci. 40 (2019) 1–30, https://doi.org/10.3390/jcs3020040.
[12] IS 801, Code of Practice for Use of Cold-Formed Light Gauge Steel Structural Members in General Building Construction, Bureau of Indian Standards, New Delhi, 1975.
[13] EN 1993-1-3, General Rules - Supplementary Rules for Cold-Formed Members and Sheeting, BSI, London, UK, 2006.
[14] IS 800, General Construction in Steel - Code of Practice, Bureau of Indian Standards, New Delhi, 2007.
[15] S.T. McKenna, T.R. Hull, The fire toxicity of Polyurethane foams, Fire Sci. Rev. 5 (2016) 1–27, https://doi.org/10.1186/s40038-016-0012-3.
[16] X. Wang, Y.-T. Pan, J.-T. Wan, D.-Y. Wang, An eco-friendly way to fire retardant flexible Polyurethane foam layer-by-layer assembly of fully bio-based substances, RSC Adv. 4 (2014) 46164–46169, https://doi.org/10.1039/c4ra07972h.
[17] Center for the Polyurethane Industry, Fire Safety Guidelines for Use of Rigid Polyurethane and Polyisocyanurate Foam Insulation in Building Construction, American Chemistry Council, Washington, 2015.